# Enhanced Nanoparticle Uptake into Virus Infected Cells: Could Nanoparticles be useful in Antiviral Therapy?

Yasmin Abo-zeid[1,4], Richard A. Urbanowicz[2,3], Brian J. Thomson [2], William L. Irving [2,3], Alexander W. Tarr[2,3], Martin C. Garnett[1]

[1]School of Pharmacy, University of Nottingham, Nottingham, NG7 2RD, UK.

[2] NIHR Nottingham Biomedical Research Centre, Nottingham University Hospitals NHS Trust and the University of Nottingham, Nottingham, UK

[3] School of Life Sciences, Faculty of Medicine & Health Sciences, Queens Medical Centre, University of Nottingham, Nottingham, NG7 2UH, UK.

[4]School of Pharmacy, Helwan University, Cairo, Egypt

**Corresponding Author:**

Yasmin Abo-zeid[1, 4]

**E-mail :** Yasmin.Abozeid@nottingham.ac.uk

**Mobile** : +44073066025

**Co-Authors:**

Richard A. Urbanowicz [2,3]

Email:Richard.Urbanowicz@nottingham.ac.uk

Brian J. Thomson[2]

Email: Brian.thomson@nottingham.ac.uk

William L. Irving[2,3]

**E-mail:** Will.Irving@nottingham.ac.uk

Alexander W. Tarr [2,3]

Email: Alex.Tarr@nottingham.ac.uk

Martin C. Garnett[1]

Email : martin.garnett@nottingham.ac.uk

**Abstract:**

Virus infections cause diseases of different severity ranged from mild infection e.g. common cold into life threating diseases e.g. Human Immunodeficiency virus (HIV), Hepatitis B. Virus infections represent 44% of newly emerging infections. Although there are many efficient antiviral agents, they still have drawbacks due to accumulation at off target organs and developing of virus resistance due to virus mutation. Therefore, developing a delivery system that can selectively target drug into affected organs and avoid off target accumulation would be a highly advantageous strategy to improve antiviral therapy. Nanoparticles (NP) can be effectively targeted to the liver, and therefore it could be used for improving therapy of hepatic virus infections including hepatitis B virus and hepatitis C virus (HCV). Many studies were performed to encapsulate antiviral agents into nano-delivery system to improve their pharmacokinetics parameters to have a better therapeutic efficacy with lower side effects. However, the effect of virus infection on the uptake of NP has not yet been studied in detail. The latter is a crucial area as modulation of endocytic uptake of nanoparticles could impact on reduce potential therapeutic usefulness of antiviral agents loaded into nano-delivery system. In this study, a fluorescently-labelled polymeric nanoparticle was prepared and used to track NP uptake into Huh7.5, human hepatoma cells transfected with replicating HCV genomes, compared with non-transfected cells as a model representing hepatocyte uptake. Confocal microscopy and flow cytometry of virus transfected Huh7.5 cells unexpectedly demonstrated two-fold increase in uptake of NP compared to non-transfected cells. Therefore, virus transfection enhanced NP uptake into Huh7.5 cells and NP could be considered as a promising delivery system for targeted treatment of hepatitis viruses..

Keywords: HCV infection, Polymer nanoparticles; Poly(glycerol adipate); Huh7.5 cells

## Introduction:

Emerging infectious diseases (EID) present a considerable threat to human life on earth. Viruses are the largest and most genetically diverse biomass on earth (Suttle, 2005) and account for 44% of EID (Taylor et al., 2001). Itaya virus, Iquitos virus, Ngari virus and Ilesha virus that are new emerging viruses in South America and East Africa (Wiwanitkit and Wiwanitkit, 2015), chikungunya virus has spread worldwide (Rothan et al., 2016), and Zika virus is now a major global health threat (Lazear and Diamond, 2016); (Paixão et al., 2016).

Emerging viruses therefore present a major public health and therapeutic challenge. Fortunately, it is known that viruses belonging to the same family, share similar characteristics (King et al., 2012). This allows many newly emerged viruses to be treated with established Food and Drug Administration (FDA) approved antiviral agents (Tan et al., 2017); (Yeo et al., 2015). Currently, there are around 90 active antiviral drugs approved for the effective treatment of many types of virus infections (Clercq, 2016). However, their administration is accompanied by side effects that can limit their potential use. E.g. ribavirin causes haemolytic anaemia (Hutchison et al., 2002), while other agents, including zidovudine, zalcitabine, lamivudine, and abacavir may give rise to peripheral neuropathy, leukopenia, pancreatitis, gout and life-threatening hypersensitivity reactions (Montessori et al., 2004). Development of antiviral resistance due to virus mutation is an additional problem (Lembo et al., 2018). Side effects are commonly due to accumulation of antiviral drug into off-target organs and therefore, finding a way that could selectively deliver antiviral agents into the target organ whilst avoiding, or reducing off-target accumulation is highly desirable and could improve the specificity and efficacy of antiviral therapy. Nano-delivery systems are known to modify the physicochemical properties e.g solubility and pharmacokinetics parameters (absorption, distribution, metabolism and elimination) of the encapsulated materials via controlled drug release. They can also be tailored for passive (e.g. controlling particle size) or active (surface decoration with

ligands) targeting of the therapeutic agents. Consequently, using a nano-delivery system for antiviral therapy could result in a lower dose of antiviral agents and a reduced side effect profile (Lembo et al., 2018). Nowacek and colleagues (Nowacek et al., 2012) prepared nanocrystals (a nano-sized delivery system composed of 100% drug with no carrier) of antiretroviral agents (Indinavir, Ritonavir, Atazanavir, and Efavirenz) as a way to improve their antiviral potency against HIV. In vitro study showed that nanocrystals improved cellular uptake into monocyte-derived macrophage (phagocytic cells) and reduced cytotoxicity compared to the free parent drug. All nanocrystals showed antiretroviral activity ranging from 20% to 100%, depending on the formulation and drug type (Nowacek et al., 2012). Although many studies have been concerned with improvement of antiviral potency and trying to reduce its side effects via encapsulation into nano-delivery system, the effect of virus infection on the uptake of NP into host cells has not been studied in detail. A down-regulation of endocytosis by virus would make NP delivery of the appropriate antiviral agent(s) less effective, whereas upregulation of endocytosis in infected cells could facilitate targeted uptake of drug into infected cells and further reduce side effects.

In order to address this important question, we used an established in vitro model of hepatitis C virus (HCV) replication to interrogate the capacity of virus infection to modulate uptake of NP. Therefore, in the current study, a fluorescently labelled polymer NP, Rhodamine B isothiocyanate (RBITC) labelled NP prepared with the bio-compatible polymer, poly(glycerol-adipate) [PGA] have been used in combination with Huh7.5 cells (non-phagocytic cells) transfected with hepatitis C virus (J6/JFH1 chimera) to track how virus infection could modulate the endocytic uptake of NP. Huh7.5 cells and the J6/JFH1 chimera have been used in the current study because it was reported that Huh7.5 cells are highly permissive to HCV infection (Lanford et al., 2003); (Sumpter et al., 2005) and the J6/JFH1 chimera (HCV RNA)

is considered as the most efficient replicating chimera in Huh7.5 cells (Lindenbach et al., 2005).

## 2. Materials and Methods:

### 2.1. Materials:

All materials were purchased from Sigma-Aldrich and VWR and used as supplied except for divinyladipate purchased from Tokyo Chemical Industry UK Ltd**.** Huh7.5, hepatocellular carcinoma cells were supplied by Apath LLC. Phenol red free - Dulbecco's Modified Eagle Medium (DMEM), foetal bovine serum (FBS), non-essential amino acids (NEAA), penicillin, streptomycin, C7-50, mouse anti-HCV core protein antibody (primary antibody) and Alexa-488, anti-mouse IgG antibody (secondary antibody) were supplied by Thermo Fisher.

### 2.2. Methods:

#### 2.2.1. Synthesis and characterisation of Poly(Glycerol adipate):

PGA is a functionalized linear polyester. It was synthesized and characterised as previously reported (Kallinteri et al., 2005); (Taresco et al., 2016). In brief, PGA was Enzymatically synthesized where equal amounts (250 mmol) of glycerol and DVA were dissolved in dry tetrahydrofuran (THF, 30 ml) in presence of a catalytic enzyme, Novozyme 435 (1.25 gm) and the reaction was stirred (overhead stirrer, 200 rpm) at constant temp (50˚C) for 24h. This was followed by enzyme filtration and evaporation of THF to obtain a yellowish jelly-like polymer.

#### 2.2.2. Preparation of fluorescently labelled nanoparticles:

RBITC PGA NP were prepared by an interfacial deposition method as reported (Meng et al., 2006) with the following modifications; RBITC (200 µl, 1 mg/ml, methanol) was added into the aqueous phase (HEPES buffer, 10 mM, pH 7.4, 7ml). The polymer (20mg) dissolved in acetone (2ml) was added dropwise into the aqueous phase while stirring. The organic solvent was evaporated overnight. RBITC PGA NP were purified by loading the sample onto a Sepharose CL-4B gel column (C2.5 X 40, Pharmacia, bed volume 91ml). The column was

eluted by water using a peristaltic pump at a flow rate of 1 ml/min and collected in fractions, 1.5ml/ tube. The peaks of dye labelled NP and free dye were detected using a Pharmacia chromatographic UV detector (206nm filter). The purified NP dispersion was collected and characterized using a Malvern Zetasizer Nano ZS (Malvern Instruments Ltd, Malvern, UK) at 25 °C ± 0.1. Particle size and zeta potential were measured in HEPES buffer (1 mM, pH 7.4) The dye loading, and encapsulation percentages were determined by a direct method. A weighed amount of freeze dried RBITC PGA NP was extracted by acetone: methanol (1:1) and dye fluorescence was measured at $\lambda_{Ex}$, 545 nm and $\lambda_{Em}$, 575 nm. Then the concentration of dye was determined from the calibration curve of known dye concentrations in acetone: methanol (1:1) using a spectrophotofluorometer (Hitachi F-4500 Hitachi, place), with slit widths adjusted to 5 nm.

**2.2.3. Stabilization of NP in physiological buffer:**

Either surfactants or human plasma were used to stabilize the RBITC PGA NP to physiological salt concentrations, (1) polysorbate surfactants (Tween 80/Tween 20) were either added to give a final concentrations 0.01% and 0.1% v/v to the pre-prepared NP (100 µl, 100 µg), or during NP preparation (*in situ* addition). (2) Alternatively, freshly isolated human plasma (100 µl) was incubated with NP (100 µl, 100 µg) for 5 minutes or 24 h before addition of phosphate buffered saline (PBS).

To investigate how PBS affects NP stability, RBITC PGA NP (100 µl, 100 µg) were diluted with PBS followed by particle size measurement in PBS. The final volume for all the previous samples was adjusted to 1 ml using PBS. For particle stability measurement, NP (100 µl) were diluted with HEPES buffer (1 mM, pH 7.4) to 1 ml and used as a control for NP size. Particle size measurements were performed using the Malvern Zetasizer Nano ZS.

**2.2.4. Investigation of NP uptake by HCV virus transfected/non-transfected Huh7.5 cells:**

Huh7.5 cells (8 x $10^6$) were electroporated in cytomix buffer (400 µl) [potassium chloride (120 mM), calcium chloride (0.15 mM), di-potassium phosphate/ Mono-potassium phosphate (10 mM, pH 7.6)] in the absence (non-transfected cells) or presence (transfected cells) of a 10 µg of J6/JFH1 HCV chimeric RNA at 220V/22ms. Cells were then incubated in phenol red free - DMEM containing 10% FBS, penicillin (100 U/ml), streptomycin (100 µg/ml), and 1% NEAA for 24 hours at 37˚C and 5% $CO_2$.

For confocal microscopy, 5 x $10^4$ of the previously electroporated cells (either virus transfected or non-transfected cells) were added to wells of a 24-well cluster (Nunclon; Nunc) containing glass cover slips. Cells were incubated for another 24 hours with phenol red free - DMEM (1 ml) followed by washing with PBS (1ml X 3). Phenol red free - DMEM (0.8 ml) and NP stabilised with FBS (100 µg, 200 µl) were added to these cells followed by incubation at 37˚C and 5% $CO_2$ for different time intervals. Cells were washed with PBS, fixed using paraformaldehyde, and then permeabilized with 0.5% TritonX-100 (400 µl) for 5 minutes. Virus core protein staining was carried out by addition of mAb C7-50 (1 µg/ml; Thermo Fisher) in PBS containing 5% FBS and incubated at room temperature (RT) for 45 minutes, followed by PBS wash (400 µl X 3). Cells were then incubated with Alexa-488 anti-mouse IgG (2 µg/ml) in 5% FBS in PBS for 60 min at RT and washed three times with PBS. Cell nuclei were stained by incubation of 5 µM 4', 6-diamidino-2-phenylindole (DAPI) in PBS with cells for 2-3 minutes at RT followed by three washes with PBS. To investigate the efficiency of virus core protein expression, a set of virus transfected /non-transfected Huh7.5 cells that were not treated with NP were prepared and processed under similar conditions, and imaged by fluorescence microscopy (Leica DMRB).

For flow cytometry quantitative studies, the previously electroporated cells (1 x $10^5$/well) either transfected or non-transfected were loaded onto 6 wells plate and incubated for another 24h. Cells were washed three times with PBS. Then, phenol red free - DMEM (3.2ml) and NP/FBS mixture, (400µg, 800µl) were added into cells followed by incubation at 37˚C and 5% $CO_2$. A set of control cells was incubated with free RBITC (5 ng, equivalent to the dye amount that might leak from RBITC PGA NP). After incubation for periods up to 4h, cells were washed three times with PBS. Cells were detached and fixed with a mixture of 4% paraformaldehyde and trypsin/EDTA (1:1) and transferred to flow cytometry tubes. Virus transfected cells were washed twice with 1% FBS in PBS (2 ml, then 1 ml) followed by centrifugation (300 g, 5 min) to remove the washing solution. Then, cells were permeabilised with PBS containing 1% FBS and 0.04% saponin (1 ml) before removal of saponin solution by centrifugation (300 g, 5 min). Cells were stained for virus core protein by incubation with C7-50 (40µg/ml) for 45 minutes at RT, washed with the saponin mixture again and incubated with anti-mouse IgG Alexa-488 (80µg/ml) for 1h at RT. Cells were washed again with the saponin mixture (1ml) and suspended in 4% paraformaldehyde. The mean fluorescence intensity (MFI) was determined using a Beckman Coulter Moflo XPD flow cytometer. Another set of virus transfected cells were incubated with NP for 4h without staining for virus to assess the possibility that permeabilization step using saponin may lead to NP release from cells. NP uptake into virus non-transfected cells was determined similarly to transfected cells but without addition of C7-50 and Alexa-488-secondary antibody. All samples were analysed in triplicate.

**2.2.5. Statistical analysis:** Statistical analysis (Two Way ANOVA) were carried out using SPSS version 21 at 95% confidence interval.

## 3. Results and Discussion:

**3.1. Synthesis and characterization of PGA:** The identity of PGA polymer was confirmed by $^{1}$H-NMR (data not shown), and size exclusion chromatography analysis gave an estimated $Mn_{,SEC}$ = 11.6 KDa and molecular weight dispersity Đ of 1.4 and molecular weight (Mw) = 16 KDa.

**3.2. Preparation and characterization of nanoparticles:**

RBITC PGA NP were prepared by a nanoprecipitation method. NP with a size around 110 nm were produced (Table 1) and had a good encapsulation efficiency percentage. Although zeta potential values indicated that particles should be stable in low ionic strength media, further investigations were carried out to ensure the particles did not aggregate under relevant physiological conditions in (see section 3.3).

**Table 1: Physicochemical characterization of RBITC PGA NP:**

| Name | Particle Size (dnm ± SD) *[PdI] | Zeta Potential (mv ± SD) | **% Load % (w/w) ± SD | ***Encapsulation Efficiency % ± SD |
|---|---|---|---|---|
| RBITC PGA NP | 110 ± 30[0.01] | - 53.7 ± 13.34 | 0.54 ± 0.13 | 54 ± 13 |

*PdI = polydispersity index, **% Load = [(Encapsulated dye weight/ NP weight) * 100]

*** % Encapsulation = [(Encapsulated dye weight/ Initial dye weight) * 100].

RBITC PGA NP was used in the current study to track the virus effect on the NP uptake into Huh7.5 cells for several reasons, (1) RBITC dye is more stable than fluorescein to quenching by light and fluorescence is improved in the acidic pH of the lysosomal compartment (Garnett and Baldwin, 1986). (2) RBITC labelled PGA NP retain their dye label for prolonged periods and so reduce possible artefacts in uptake studies as was demonstrated earlier in our group (Meng et al., 2006) (3) The initial RBITC released from NP in culture medium over 24h was very low (4.5%) (Meng et al., 2006) (4) Polymer biocompatibility and biodegradability is important to be considered for the future therapy of polymer based nano-delivery system. The

degradation by-products of PGA are adipic acid and glycerol which are safe compounds as approved by FDA (Zhang et al., 2014) (5) The cytotoxicity of PGA has been determined earlier in our group (Kallinteri et al., 2005), and it showed a very low cell toxicity against Human Leukaemia cell line, HL60 cell and Human liver cell lines, HepG2 cells at the top dose of polymer NP, 100 times more of polymer amount required for a therapeutic nano-delivery system. Also, Navarro and his colleagues (Navarro et al., 2017) have used PGA elastomer and it was demonstrated to be non-cytotoxic to embryonic mouse fibroblasts (NIH/3T3) after seeding cells for 6 hours over PGA discs .

**3.3. Particle stabilization in physiological buffer:**

Particles incubated with PBS showed a high level of aggregation, (Figure 1). Although different concentrations of polysorbate surfactants were used as potential stabilisers, they were not accompanied by any improvement of particle stability (data not shown). However, 24h incubation with human plasma stabilized particles successfully in PBS, resulting in particle sizes ranging from 237 to 300 nm in diameter (Figure 1). A small peak of higher particle size in DLS (data not shown) was noted indicating some aggregate formation (representing 14% of low particle size peak by intensity).

The stability of NP in biological systems is an important consideration, as particles in solutions with physiological salt concentrations and pH values can form micrometer-sized coarse agglomerates (Deguchi et al., 2007); (Murdock et al., 2008). Coarse agglomerates of NP will behave differently in a biological system compared to well-dispersed NP, especially with respect to endocytic uptake of particles (Buford et al., 2007). The effectiveness of human plasma in preventing aggregation could be explained by adsorption of protein molecules onto the NP surface forming a protein corona (Lynch and Dawson, 2008) that is able to prevent particle aggregation (Gebauer et al., 2012). The improvement of NP stabilization after 24h incubation with human plasma might be due to a better and more efficient coating of NP by

plasma protein that was not achieved by a short incubation. This suggested a relatively slow adsorption or slow equilibration process of plasma protein adsorption onto the surface of NP (Casals et al., 2010). This is consistent with the study of Bihari et al, who demonstrated that human, bovine and mouse serum albumins offered a better stability than Tween 80 for different types of NP, TiO2 (rutile), ZnO, Ag (silver), and carbon nanotubes in PBS. In addition, mouse serum achieved a similar stabilizing effect to that achieved by pure mouse serum albumin (Bihari et al., 2008). Therefore, incubation of particles with plasma for 24h was the method used to stabilize the particles for subsequent studies.

### 3.4. Investigation of virus core protein expression after Huh7.5 cells transfection with J6/JFH1 HCV chimera:

Fluorescence Microscopy was used to assess active replication in Huh7.5 cells transfected with HCV genomes. Expression of virus core protein was detected 48h after transfection of Huh7.5 cells with J6/JFH1 and staining of the core protein using the primary antibody, C7-50 and secondary antibody- Alexa488 (Figure 2). The green fluorescence observed in Figure 2B represents expression of HCV core protein. Different cells were observed to have varying levels of Core expression (Figure 2B). A flow cytometry study (Figure 3) was also performed to assess virus transfection of Huh7.5 cells. Figure (3A) is the flow cytometry histogram, where X–axis represents Alexa-488 fluorescence intensity and it is indicative of labelled virus core protein and therefore it reflects the efficiency of virus transfection while Y-axis represents the number of events (number of cells).

The red, black and blue histograms are blank1 (electroporated non-transfected Huh7.5 cells), blank2 (electroporated non-transfected Huh7.5 cells, treated with primary and secondary antibodies, to investigate if there a possibility of non-specific binding) and experimental (electroporated transfected Huh7.5 cells, treated with primary and secondary antibodies) respectively. As seen from the histogram, the red peak (Blank 1) represents the background

fluorescence of cells. It was found that there is a limited non-specific binding of antibodies as revealed by slight shift of red peak to a black peak (Blank 2) of higher fluorescence intensity along the Alexa-488 axis. Blue peak (Experimental sample to demonstrate virus replication) has the highest fluorescence signal of Alexa-488 and this is indicative of virus transfection success. However, not all cells in the blue peak replicated virus equally and this could be demonstrated by division of blue peak into 3 sub-peaks: two small sub-peaks and a larger sub-peak. A small sub-peak with a very low fluorescence signal ranging from 1 to 10 represents a cell population that did not replicate virus. The second small sub-peak and the larger sub-peak represent cell populations that replicated virus but with unequal efficiency, where the small sub-peak with signal fluorescence ranging from 150 to 10,000 along Alexa-488 axis represents the cell population with the highest efficiency of virus replication while the larger peak had a lower fluorescence intensity with signal intensity ranging from 10 to 150.

Moving to flow cytometry graphs Figure 3 (B), (C), (D) representing Blank1, Blank2, and Experimental respectively. X-axis represent the Alexa-488 fluorescence intensity which is indicative of labelled virus core protein while Y-axis represent RBITC fluorescence intensity that is indicative of NP uptake. Each graph is subdivided into 4 quadrants where the lower left (LL) quadrant represents cells with a low fluorescence signal for both RBITC and labelled virus core protein. Moving from LL quadrant to the lower right (LR) quadrant indicates an increase of Alexa-488 fluorescence intensity that is indicative of virus transfection. As shown in Figure 3 (B), for blank1, almost all cells in the population occupied the LL quadrant with a very limited number of cells (0.26%) appearing in the LR quadrant. Figure 3 (C) represents blank2 cells where cells occupied the same quadrants as blank1 but more cells occupied LR (0.58) and this is indicative of slightly more cells with higher fluorescence intensity for Alexa-488. This might reflect a non-specific binding due to treatment with primary and secondary

antibodies. Figure 3 (D), represents Experimental (transfected cells) where cells occupy both LL and LR quadrants but LR quadrant has a higher population of cells (13.9%) than both blank 1 and blank 2. This demonstrated that virus transfection of Huh7.5 cells was successful due to higher number of cells with higher fluorescence intensity along Alexa-488 axis. However, as previously described in the flow cytometry histogram Figure 3 (A) that most cells are transfected with (J6/JFH1) but not all cells equally replicated the virus. The latter means that cells located in LL quadrant in graph (D) might contain some cells that are infected by Huh7.5 cells but do not replicate efficiently enough to be detected in LR quadrant. Although, not all cells replicate virus equally, the transfected cells could be used to investigate the effect of virus transfection on the uptake of RBITC PGA NP.

**3.5. Confocal microscopy investigation of NP uptake by virus transfected Huh7.5 cells versus non-transfected cells:**

The time course of NP uptake into transfected cells was initially investigated by confocal microscopy (Figure 4). A, B, C and D images represent blue, green, red fluorescence channels and overlay of all channels respectively of a single plane image of transfected cells incubated with NP. The red fluorescence shows RBITC PGA NP. After 0.5 h incubation, red fluorescence was seen as fine dots distributed across the cells. With increasing incubation time, the number of fine dots first increased, and then larger bright patches of red fluorescence were seen after 2h. By 4 h, there was a high level of both fine dots and patches. Some red fluorescence patches of aggregated particles that were not associated with cells could also be seen (green arrows).

A closer examination of the fluorescence distribution in the cells at different depth through the cells (different Z-stacks) by confocal microscopy is presented (Figure 5). The presence of red fluorescence in the plane of the section through the nucleus demonstrated an intracellular localisation of the particles. The appearance of these dots close to the peri-nuclear region together with an increase of the fluorescence intensity over incubation time suggested that

uptake of NP by cells was a continuous endocytic process where endosomes fused together to form late endosomes that are further fused to form lysosomes. It is generally accepted that most nano-particulates are taken up into cells by a variety of endocytic routes (Garnett and Kallinteri, 2006). The physicochemical properties of NP and culture medium have a role on the interaction of NP with cells. PGA polymer has COOH group that should be in the anion form at the pH (7.4) of the culture medium and therefore RBITC PGA NP should carry negative charge as revealed by its zeta potential value measured at pH 7.4 (HEPES buffer, 10mM), (- 53.7 ± 13.34). upon addition of RBITC PGA NP into the culture medium, protein -corona will be formed due to adsorption of different types of proteins and this should facilitate their uptake into cells. This is consistent with the literature where carboxylated polystyrene particles (1µm and 50nm) were taken up by alveolar type I cells (Fröhlich, 2012) . Park and his colleagues (Park et al., 2011) prepared gold NP functionalized with aromatic thiol derivatives to produce nanoparticles with a surface functional groups; NH2, COOH and OH. Functionalized gold NP were able to adsorb proteins and had been taken up into A549 cells, adenocarcinomic human alveolar basal epithelial cells. It has been shown that there is not much difference of cell uptake due to different surface groups due to thick protein corona formed (Park et al., 2011). Therefore, it is the adsorbed layer of protein which affects NP uptake into cells rather than the charge of the naked particles. The uptake of RBITC PGA NP into Huh7.5 cells is also in agreement with a previous publication reporting that RBITC PGA NP are endocytosed and sorted into the lysosomal compartment of DAOY cells, a human medulloblastoma cell line (Meng et al., 2006).

A single plane confocal microscopy image of NP taken up by virus-transfected cells compared to non-transfected cells after incubation for 4 h is presented (Figure 6). Non-transfected cells (Figure 6A) showed a relatively small number of fine dots of red fluorescence (orange arrow) that were associated with the cells compared to the significantly coarser and brighter dots seen

in the virus transfected cells (Figure 6B). The red fluorescence observed outside cells suggested some extracellular particle aggregation had occurred (green arrows).

### 3.6. Flow Cytometry quantitative study of NP uptake by virus transfected and non-transfected Huh7.5 cells:

Flow cytometry of NP uptake into virus transfected and non-transfected Huh7.5 cells over different incubation times (0 to 4 h) was performed (Figure 7). The X-axis represents Alexa-488 fluorescence intensity (indicative of virus transfection) while the Y-axis represents RBITC fluorescence intensity (indicative of NP uptake). The control graph shows that the majority of cells have a small shift along the X-axis demonstrating virus transfection. However, there are smaller populations with no increase or a little increase of fluorescence due to labelled core proteins of the virus as previously described in section 3.4. With increasing incubation time there was a progressive increase in fluorescence on the Y-axis representing NP uptake for the majority of the cell population in both transfected and non-transfected cells. For cells electroporated with HCV there was a significant population of cells with either no significant virus transfection or a low virus transfection in which no increase in NP fluorescence was observed. This might be due to an effect of virus RNA on cell vitality and this requires further investigation to determine whether these cells die or resume endocytosis at a later time. For non-transfected cells, there is very small population of cells showing low NP uptake.

For better understanding of these results, it should be noted that the FACS had been set up to avoid the fluorescence spill over from RBITC channel into Alexa-488 channel and vice versa. The FACS had been set up using Huh7.5 cells of different properties in the following order; (1) Huh7.5 cells; non-transfected cells that were not treated with NP and they were used to blank the FACS. (2) a set of Huh7.5 cells; non-transfected and treated with NP to adjust red channel, (3) a set of Huh7.5 cells; transfected and not treated with NP to adjust green channel and (4) a set Huh7.5 cells; transfected and treated with NP to avoid spill over of fluorescence.

The data of fluorescence of Alexa-488 versus fluorescence of RBITC is presented (Figure 7) to show that the increased fluorescence from nanoparticle uptake, is related to the fluorescence from virus transfection. The relative proportion of cells (percentage of gated cells in each quadrant) involved in both virus transfection and nanoparticle uptake is also presented (Table 2). The fluorescence from virus transfection is confined to the right half of the graph (Figure 7) and (LR and UR in Table 2), and the fluorescence from particle uptake is found in the upper half of the graph (Figure 7) and (UL and UR in table 2). Looking at percentages of cells in different quadrants (Table 2), we can see that most of the non-transfected cells did show uptake of nanoparticles (UL quadrant). In contrast, in the transfected cells there was a much lower percentage of cells in the UL quadrant, but also significant number of cells which show virus transfection and NP uptake (UR quadrant), and non-transfected and no NP uptake (LL quadrant). These changes in the numbers of cells in these quadrants show that virus transfection did influence NP uptake. It should also be noted, as explained earlier (Figure 3) that some of Huh7.5 cells replicate virus to a lower efficiency and might occupy the LL quadrant. From the above, we could speculate that the statistics of cells (% Gated cells) presented in Table 2 may underestimate the population of transfected cells in the LR quadrant and may overestimate the true percentage of cells in the LL quadrant because of this population of cells with a lower efficiency of transfection showing a low fluorescence of virus expression. Therefore, the NP uptake detected in UL quadrant for transfected cells might involve NP uptake not only due to non-transfected cells but also, virus transfected cells that replicate virus with a lower efficiency.

Quantitative flow cytometry of NP uptake by virally transfected/non-transfected Huh7.5 cells is presented (Figure 8). NP uptake by virus transfected cells was significantly higher ($P < 0.05$) than non-transfected cells over all incubation time intervals, around 2 times more. It is also interesting to note that the rates of uptake changed with time and the change in rates of uptake

Table 2: % Gated cells for virus transfected and non-transfected Huh7.5 cells

| **Time** | ***%Gated for virus transfected Cells*** | | | | ***%Gated for virus non-transfected cells*** | | | |
|---|---|---|---|---|---|---|---|---|
| | LL | UL | LR | UR | LL | UL | LR | UR |
| **Experimental** | 99.34 | 0.03 | 0.58 | 0.05 | - | - | - | - |
| **0** | 31.38 | 51.64 | 4.30 | **12.67** | 27.14 | 72.53 | 0.11 | **0.22** |
| **0.5** | 13.74 | 66.77 | 1.65 | **17.84** | 2.46 | 97.17 | 0.09 | **0.29** |
| **1** | 14.15 | 67.82 | 1.60 | **16.42** | 1.47 | 98.11 | 0.09 | **0.32** |
| **2** | 13.03 | 67.32 | 1.43 | **18.22** | 1.46 | 97.91 | 0.13 | **0.51** |
| **3** | 11.10 | 69.18 | 0.82 | **18.90** | 1.09 | 98.46 | 0.07 | **0.38** |
| **4** | 10.78 | 68.60 | 0.91 | **19.70** | 1.04 | 98.50 | 0.07 | **0.39** |

Experimental: Cells electroporated in presence of HCV RNA and treated with 1ry and 2ry antibodies
LL: Lower Left quadrant; low virus transfection, low NP uptake
UL: Upper Left quadrant; low virus transfection, raised NP uptake
LR: Lower Right quadrant; raised virus transfection, low NP uptake
UR: Upper Right quadrant; raised virus transfection, raised NP uptake

differed between transfected and non-transfected cells. In non-transfected cells the rate of uptake was constant for about 2h before the rate started to drop off. However, in virus transfected cells there was a reduction in rate of uptake after a very rapid initial rate for the first hour of incubation. After this initial period the rate of uptake showed a value similar to the initial rate of uptake in non-transfected cells and this rate is then maintained for the remainder of the 4h period.

There was a slow rate of release of free RBITC from NP, and a control sample representing the amount of free dye associated with NP was also assessed. Free dye uptake was negligible after incubation with either virus transfected or non-transfected cells for 4 h and this demonstrated that fluorescence measured was due to actual NP uptake. The latter is in agreement with a

previous publication that reported incubation of free dye (RBITC) with DAOY cells was associated with a very limited uptake compared to RBITC PGA NP (Meng et al., 2006). The staining for virus core protein required membrane permeabilization by saponin, which could potentially result in some leakage of NP. To account for this, control samples where cells were incubated with NP but not permeabilised was assessed. There was no statistically significant difference in uptake between permeabilised and non-permeabilised cells (Figure 8). The enhancement of NP uptake due to virus transfection might be explained by enhancement of one or more of the endocytic pathways that are responsible for NP uptake. This is consistent with the previous finding that adenovirus infection enhanced macro-pinocytosis process due to modulation of the cell cytoskeleton (Meier et al., 2002). The selective advantage of NP uptake into virus transfected hepatocytes as presented in the current study offers a significant benefit that might be attained by encapsulating antiviral agents for hepatic virus infection e.g. Hepatitis B and Hepatitis C. This concept could be further extended to other viruses, but further investigations is essential.

## 4. Conclusions:

Drug delivery using nanoparticles has been of interest since the early 1980s, but more recently there have been significant advances in drug delivery using biodegradable nanoparticles. Much of this interest in nanoparticle delivery systems has its focus on cancer treatment because of the enhanced permeability and retention effect which provides a mechanism for selective delivery or increased targeting to tumour tissue. We have additionally reported that under certain conditions PGA particles also showed an enhanced uptake into DAOY medulloblastoma cells in cells culture. There are other tissues where possibilities exist for targeting of nanoparticles and which may be exploited therapeutically. One such possibility is delivery to the liver. With this in mind we hypothesised that nanoparticle delivery may be a

good way to enhance delivery of antiviral agents to the liver while reducing the off-target accumulation and therefore side effects of antiviral agents in case of virus liver infections e.g. hepatitis B and C viruses.

The current work demonstrated that Huh7.5 cells, a hepatic cell line transfected with HCV RNA showed a higher NP uptake than non-transfected cells. Virus transfection also resulted in changes in rates of uptake with time in comparison to non-transfected cells. These data suggest that polymer nanoparticles may provide a useful future delivery system for targeting virus infections of liver providing that antiviral agents could be sufficiently loaded into polymer nanoparticles. This approach could prove particularly effective in eradication of hepatitis B virus, where elimination of the HBV covalently closed circular DNA requires selective targeting of molecular therapies to latently infected hepatocytes. The application of NP directed therapies for other important viral diseases is an exciting possibility that requires further exploration.

## 5- Declaration of Interest

The authors declare no conflicts of interest

**Acknowledgment:** Yasmin Abo-zeid was funded by a studentship from the Egyptian Culture Centre and Educational Bureau. Huh7.5 cells and the J6/JFH1 chimeric virus was a gift from Apath L.L.C.

## References

Bihari, P., Vippola, M., Schultes, S., Praetner, M., Khandoga, A.G., Reichel, C.A., Coester, C., Tuomi, T., Rehberg, M., Krombach, F., 2008. Optimized dispersion of nanoparticles for biological in vitro and in vivo studies. Part. Fibre Toxicol. 5, 1–14. https://doi.org/10.1186/1743-8977-5-14

Buford, M.C., Jr, R.F.H., Holian, A., 2007. A comparison of dispersing media for various engineered carbon 9, 1–9. https://doi.org/10.1186/1743-8977-4-6

Casals, E., Pfaller, T., Duschl, A., Oostingh, G.J., Puntes, V., 2010. Time Evolution of the Nanoparticle Protein Corona 4, 3623–3632.

Clercq, E. De, 2016. Approved Antiviral Drugs over the Past 50 Years 29, 695–747.

https://doi.org/10.1128/CMR.00102-15.Address

Deguchi, S., Yamazaki, T., Mukai, S., Usami, R., Horikoshi, K., 2007. Stabilization of C 60 Nanoparticles by Protein Adsorption and Its Implications for Toxicity Studies 60, 854–858.

Fröhlich, E., 2012. The role of surface charge in cellular uptake and cytotoxicity of medical nanoparticles 5577–5591.

Garnett, M.C., Baldwin, R.W., 1986. Endocytosis of a monoclonal antibody recognising a cell surface glycoprotein antigen visualised using fluorescent conjugates 221, 214–221.

Garnett, M.C., Kallinteri, P., 2006. Nanomedicines and nanotoxicology: Some physiological principles. Occup. Med. (Chic. Ill). 56, 307–311. https://doi.org/10.1093/occmed/kql052

Gebauer, J.S., Malissek, M., Simon, S., Knauer, S.K., Maskos, M., Stauber, R.H., Peukert, W., Treuel, L., 2012. Impact of the Nanoparticle − Protein Corona on Colloidal Stability and Protein Structure.

Hutchison, J.G.M.C., Manns, M., Patel, K., Poynard, T., Lindsay, K.L., Trepo, C., Dienstag, J., Lee, W.M., Mak, C., Garaud, J.J., Albrecht, J.K., The, F.O.R., Hepatitis, I., 2002. Adherence to Combination Therapy Enhances Sustained Response in Genotype-1–Infected Patients With Chronic Hepatitis C 1061–1069. https://doi.org/10.1053/gast.2002.35950

Kallinteri, P., Higgins, S., Hutcheon, G.A., Pourc, C.B.S., Garnett, M.C., 2005. Novel Functionalized Biodegradable Polymers for Nanoparticle Drug Delivery Systems 1885–1894.

King, A.M.Q., Adams, M.J., Carstens, E.B., Lefkowitz, E.J., 2012. Virus Taxonomy: Ninth Report of the International Committee on Taxonomy of Viruses.

Lanford, R.E., Guerra, B., Lee, H., Averett, D.R., Pfeiffer, B., Chavez, D., Notvall, L., Bigger, C., 2003. Antiviral Effect and Virus-Host Interactions in Response to Alpha Interferon , Gamma Interferon , Poly ( I ) -Poly ( C ), Tumor Necrosis Factor Alpha , and Ribavirin in Hepatitis C Virus Subgenomic Replicons 77, 1092–1104. https://doi.org/10.1128/JVI.77.2.1092

Lazear, H.M., Diamond, M.S., 2016. Zika Virus: New Clinical Syndromes and Its Emergence in the Western Hemisphere. J. Virol. 90, 4864–4875. https://doi.org/10.1128/JVI.00252-16

Lembo, D., Donalisio, M., Civra, A., Argenziano, M., Lembo, D., Donalisio, M., Civra, A., Argenziano, M., 2018. Expert Opinion on Drug Delivery Nanomedicine formulations for the delivery of antiviral drugs : a promising solution for the treatment of viral infections. Expert Opin. Drug Deliv. 15, 93–114. https://doi.org/10.1080/17425247.2017.1360863

Lindenbach, B.D., Evans, M.J., Syder, A.J., Tellinghuisen, T.L., Liu, C.C., Mckeating, J.A., Rice, C.M., 2005. Complete Replication of Hepatitis C Virus in Cell Culture 623–627.

Lynch, I., Dawson, K.A., 2008. The key role of protein-nanoparticle interactions in nanomedicine and 3, 40–47.

Meier, O., Boucke, K., Hammer, S.V., Keller, S., Stidwill, R.P., Hemmi, S., Greber, U.F., 2002. Adenovirus triggers macropinocytosis and endosomal leakage together with its clathrin-mediated uptake 158, 1119–1131. https://doi.org/10.1083/jcb.200112067

Meng, W., Parker, T.L., Kallinteri, P., Walker, D.A., Higgins, S., Hutcheon, G.A., Garnett, M.C., 2006. Uptake and metabolism of novel biodegradable poly ( glycerol-adipate ) nanoparticles in DAOY monolayer 116, 314–321. https://doi.org/10.1016/j.jconrel.2006.09.014

Montessori, V., Press, N., Harris, M., Akagi, L., Montaner, J.S.G., 2004. Adverse effects of

antiretroviral therapy for HIV infection 170, 229–238.

Murdock, R.C., Braydich-stolle, L., Schrand, A.M., Schlager, J.J., Hussain, S.M., Al, M.E.T., 2008. Characterization of Nanomaterial Dispersion in Solution Prior to In Vitro Exposure Using Dynamic Light Scattering Technique 101, 239–253. https://doi.org/10.1093/toxsci/kfm240

Navarro, L., Ceaglio, N., Rintoul, I., 2017. Structure and properties of biocompatible poly ( glycerol adipate ) elastomers modi fi ed with ethylene glycol. Nat. Publ. Gr. 1–8. https://doi.org/10.1038/pj.2017.30

Nowacek, A.S., Balkundi, S., Mcmillan, J., Roy, U., Martinez-, A., Mosley, R.L., Kanmogne, G., Kabanov, A. V, Gendelman, H.E., 2012. NIH Public Access 150, 204–211. https://doi.org/10.1016/j.jconrel.2010.11.019.Analyses

Paixão, E.S., Barreto, F., Da Glória Teixeira, M., Da Conceição N Costa, M., Rodrigues, L.C., 2016. History, epidemiology, and clinical manifestations of Zika: A systematic review. Am. J. Public Health 106, 606–612. https://doi.org/10.2105/AJPH.2016.303112

Park, J., Park, J., Park, J., Park, J., Ock, K., Ganbold, E., Woong, N., Cho, K., 2011. Preferential adsorption of fetal bovine serum on bare and aromatic thiol- functionalized gold surfaces in cell culture media Journal of Colloid and Interface Science Preferential adsorption of fetal bovine serum on bare and aromatic thiol-functionalized g. J. Colloid Interface Sci. 363, 105–113. https://doi.org/10.1016/j.jcis.2011.07.006

Rothan, H.A., Bahrani, H., Abdulrahman, A.Y., Mohamed, Z., Teoh, T.C., Othman, S., Rashid, N.N., Rahman, N.A., Yusof, R., 2016. Mefenamic acid in combination with ribavirin shows significant effects in reducing chickungunya virus infection in vitro and in vivo. Antiviral Res. https://doi.org/10.1016/j.antiviral.2016.01.006

Sumpter, R.J., Loo, Y.-M., Foy, E., Li, K., Yoneyama, M., Fujita, T., Lemon, S.M., Michael Gale, J., 2005. Regulating Intracellular Antiviral Defense and Permissiveness to Hepatitis C Virus RNA Replication through a Cellular RNA Helicase, RIG-I 79, 2689–2699. https://doi.org/10.1128/JVI.79.5.2689

Suttle, C.A., 2005. Viruses in the sea 437. https://doi.org/10.1038/nature04160

Tan, M.J.A., Gaunt, M.W., Hibberd, M.L., Nicholas Furnham, 2017. The complex relationship between the emerging flaviviruses : dengue and Zika 18–21.

Taresco, V., Creasey, R.G., Kennon, J., Mantovani, G., Alexander, C., Burley, J.C., Garnett, M.C., 2016. Variation in structure and properties of poly ( glycerol adipate ) via control of chain branching during enzymatic. Polymer (Guildf). 89, 41–49. https://doi.org/10.1016/j.polymer.2016.02.036

Taylor, L.H., Latham, S.M., Woolhouse, M.E.J., 2001. Risk factors for human disease emergence. https://doi.org/10.1098/rstb.2001.0888

Wiwanitkit, S., Wiwanitkit, V., 2015. Journal of Tropical Diseases Some New Emerging Viral Diseases in South America and East Africa : The 3, 2–3. https://doi.org/10.4172/2329-891X.1000160

Yeo, K.L., Chen, Y., Xu, H.Y., Dong, H., Wang, Q., Yokokawa, F., Shi, P., 2015. Synergistic Suppression of Dengue Virus Replication Using a Combination of Nucleoside Analogs and Nucleoside Synthesis 59, 2086–2093. https://doi.org/10.1128/AAC.04779-14

Zhang, T., Howell, B.A., Dumitrascu, A., Martin, S.J., Smith, P.B., 2014. Synthesis and characterization of glycerol-adipic acid hyperbranched polyesters. Polymer (Guildf). 55, 5065–5072. https://doi.org/10.1016/j.polymer.2014.08.036

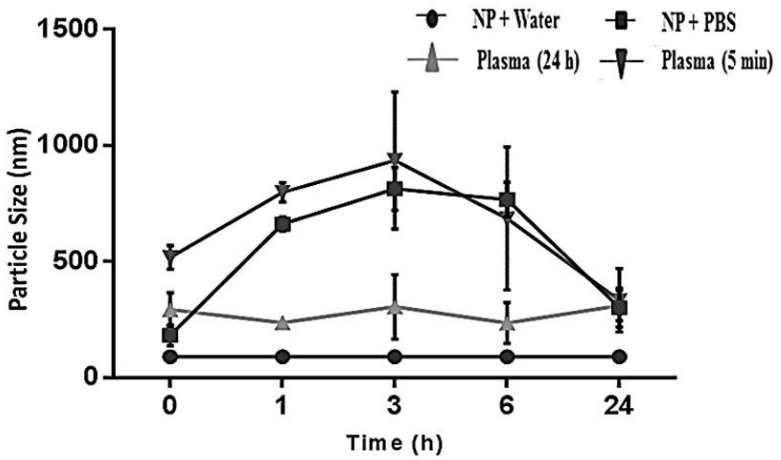


**Figure 1: Effect of human plasma proteins on stability of RBITC PGA NP;** The stability of NP in PBS was determined over 24h by particle size measurement using Malvern Zetasizer Nano ZS. NP showed a massive aggregation in PBS. However, incubation of particles with human plasma for 24h improved particle stability in PBS. Error bars represent SD.

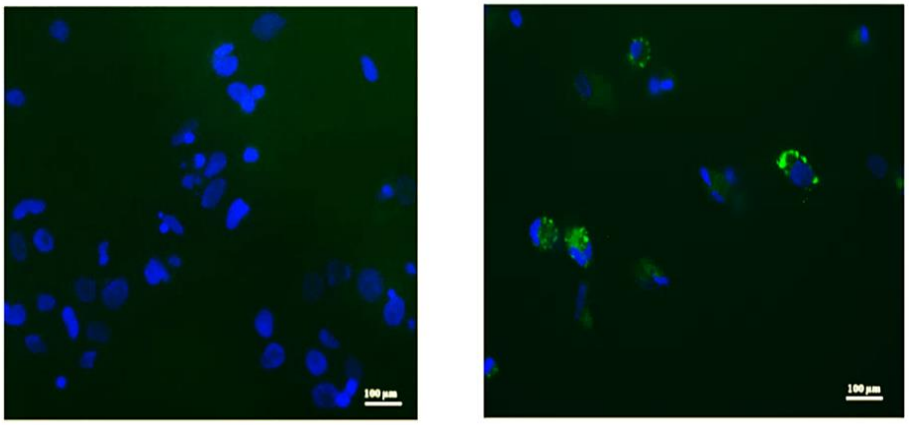


A B

**Figure 2: Fluorescence microscopy images of non-transfected/transfected Huh7.5 cells;** Cells electroporated in absence of HCV RNA (J6/JFH1) (A) and in presence of J6/JFH1(B). Blue fluorescence represents nuclei stained with DAPI and the green fluorescence represents presence of HCV core protein. Images showed that virus has replicated and produced viral core protein.

569

570

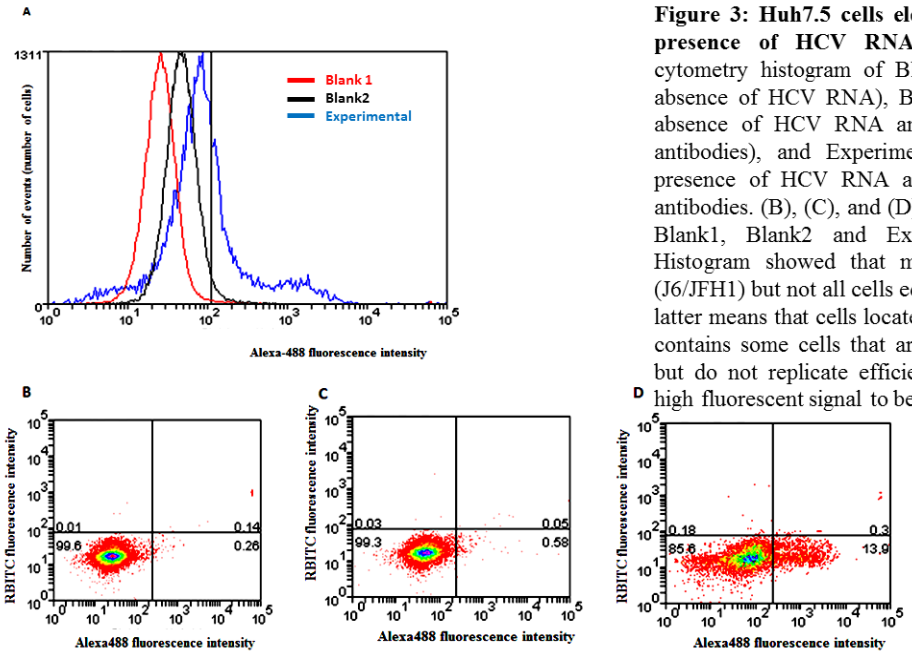


**Figure 3: Huh7.5 cells electroporated in absence and presence of HCV RNA (J6/JFH1);** (A) the flow cytometry histogram of Blank1 (cells electroporated in absence of HCV RNA), Blank2 (cells electroporated in absence of HCV RNA and treated with 1ry and 2ry antibodies), and Experimental (cells electroporated in presence of HCV RNA and treated with 1ry and 2ry antibodies. (B), (C), and (D) are flow cytometry graphs of Blank1, Blank2 and Experimental respectively. (A) Histogram showed that most cells are transfected by (J6/JFH1) but not all cells equally replicated the virus. The latter means that cells located in LL quadrant in graph (D) contains some cells that are transfected by Huh7.5 cells but do not replicate efficiently enough to be produce a high fluorescent signal to be detected in LR quadrant.

571

572

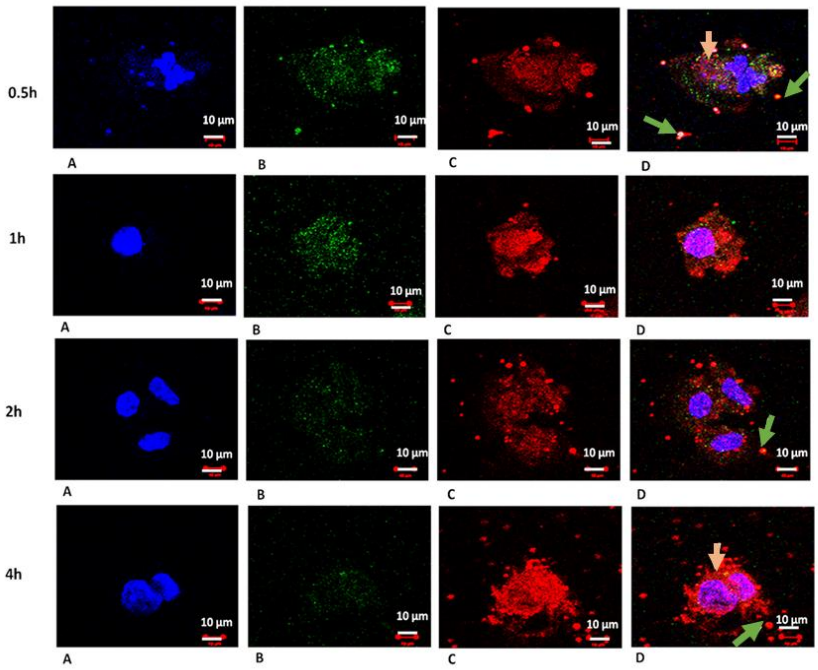


**Figure 4: Time course of Nanoparticle uptake into HCV transfected Huh7.5 cells;** Confocal microscopy images of J6/JFH1 transfected Huh7.5 cells after incubation with RBITC PGA NP for different time intervals (0.5 to 4h) at 37°C and 5% $CO_2$. A, B, C, and D images are blue, green, red channels and overlay of all channels respectively. Blue fluorescence represents nuclei stained with DAPI, green fluorescence indicates labelled virus core protein and the red fluorescence represents RBITC PGA NP. Initially, cell associated NP appeared as fine red dots finely dispersed across the cell which became coarser and associated with the peri-nuclear region as time progressed (orange arrow). Some extracellular aggregated particles were present (green arrows). Scale bar is 10 µm.

573

574

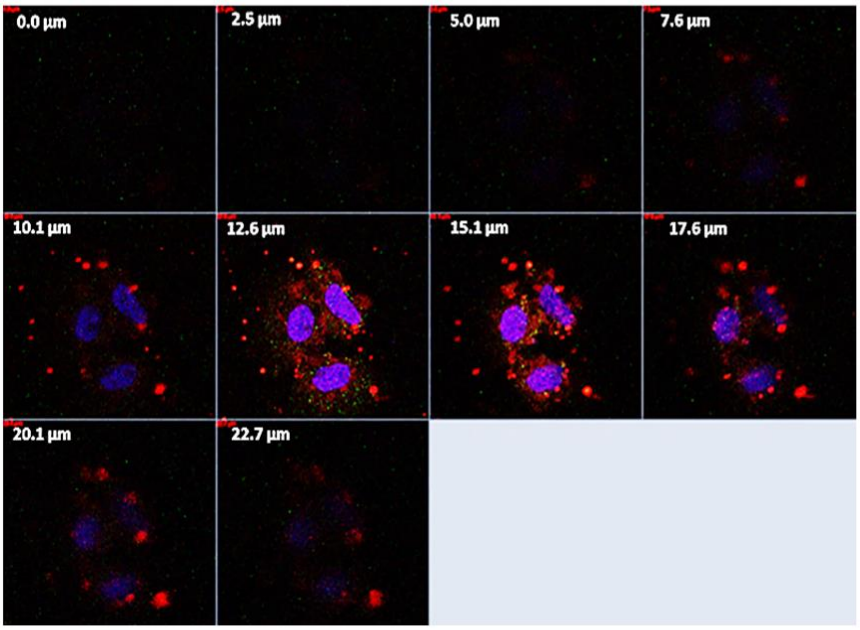


**Figure 5: Intracellular localisation of Nanoparticles in J6/JFH1 Transfected Huh7.5 cells;** Confocal microscopy images at different Z-planes (depth across cells) of transfected Huh7.5 cells after incubation for 2 h with RBITC PGA NP at 37℃ and 5% $CO_2$. Blue fluorescence represents nuclei stained with DAPI. Green fluorescence represents labelled virus core protein and red fluorescence represents NP. The figures show the height in the Z-stack. The red fluorescence coincident with the blue fluorescence of the nuclei is indicative that NP are inside cells.

575

576

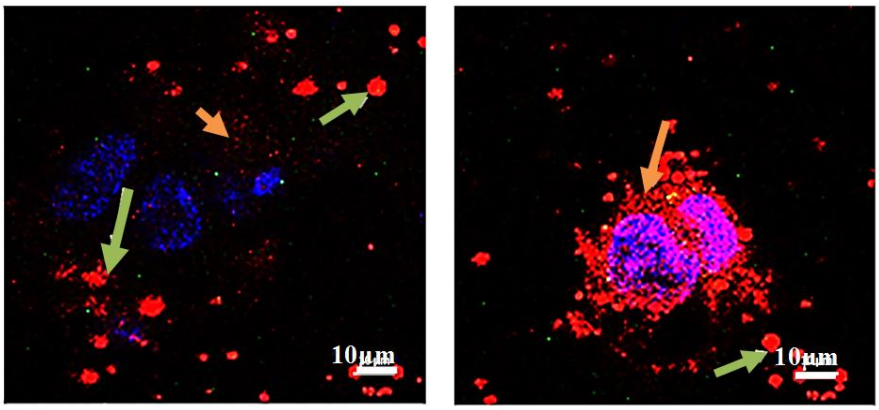


**Figure 6: Comparison of nanoparticle uptake into J6/JFH1 transfected versus non-transfected cells;** Confocal microscopy images of non-transfected (A) and transfected (B) Huh-7.5 cells incubated for 4 h with RBITC PGA NP at 37℃ and 5% $CO_2$; Blue fluorescence represents nuclei stained with DAPI; red fluorescence represents RBITC PGA NP taken up by cells (yellow arrows). Red fluorescence in transfected cells was brighter than in non-transfected cells. This indicates that virus infection enhanced NP uptake. Green arrows represent aggregated particles outside the cells, scale bar is 10 µm.

577

578

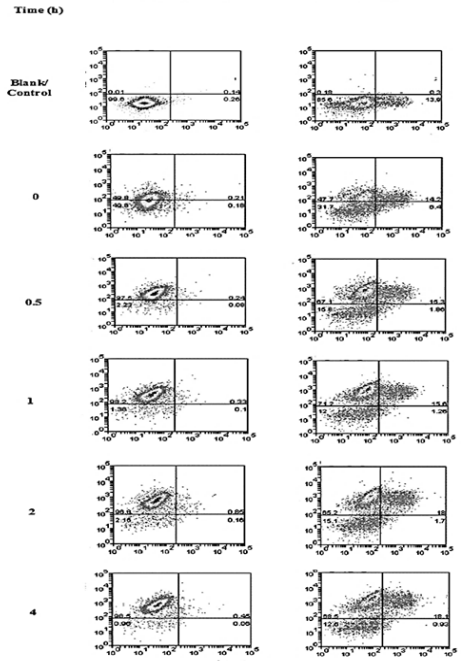


**Figure 7: Flow cytometry analysis of Nanoparticle uptake into Huh7.5 cells;** Flow cytometry graphs of Huh7.5 cells incubated with RBITC PGA NP for different time intervals where X-axis represents Alexa-488 fluorescence intensity; Y-axis represents RBITC fluorescence. Left column, J6/JFH1 non-transfected cells, right column, J6/JFH1 transfected cells. Blank cells (the top graph of left column) represent electroporated non-transfected cells that were not incubated with NP while control cells (the top graph of right column) represent electroporated transfected cells that were not incubated with NP. Cells show NP uptake as indicated by movement of signals from lower quadrants to upper quadrants where non-transfected cells show in the left-hand quadrants and transfected cells in the right-hand quadrants. In the transfected cells there is a small population of cells that did not take up NP.

579

580

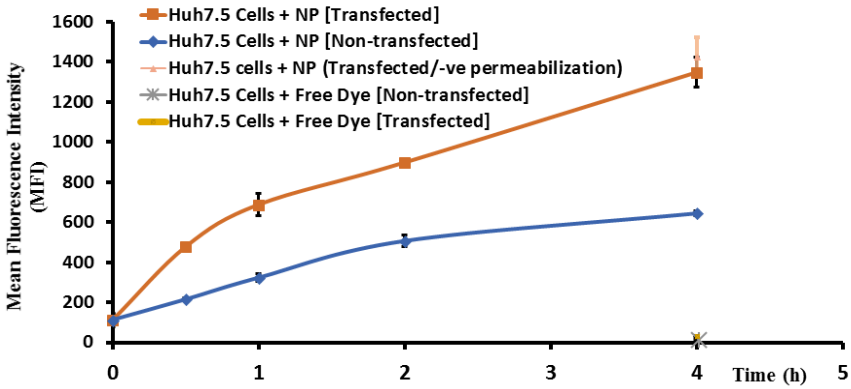


**Figure 8: Quantitation of Nanoparticle uptake into non-transfected versus transfected Huh7.5 human hepatoma cells by flow cytometry;** Mean Fluorescence Intensity (MFI) was recorded for transfected and non-transfected cells incubated with fluorescently labelled polymer NP at 37° C and 5%$CO_2$ for different time intervals (0 upto 4 h): Rate of NP uptake by transfected cells was much higher than non-transfected cells. MFI is due to NP uptake rather than free dye uptake that might associate NP as indicated by very low MFI recovered from free dye incubated with cells for 4 h. Permeabilization process to label virus core protein was not associated with leakage of NP as indicated by similar MFI at 4h for transfected cells (cells exposed to permeabilization process) and transfected (-ve permeabilization). Error bars represent SD.

581